Title
HYDRODYNAMICS AND MASS TRANSFER IN A POROUS-WALL CHANNEL

Authors
Lessner, P.
Newman, J.

Publication Date
1983-08-01

Lawrence Berkeley Laboratory

UNIVERSITY OF CALIFORNIA

APPLIED SCIENCE DIVISION

Submitted to the Journal of the Electrochemical Society

HYDRODYNAMICS AND MASS TRANSFER IN A POROUS-WALL CHANNEL

P. Lessner and J. Newman

August 1983

APPLIED SCIENCE DIVISION

Prepared for the U.S. Department of Energy under Contract DE-AC03-76SF00098

LBL-16568

HYDRODYNAMICS AND MASS TRANSFER IN A POROUS-WALL CHANNEL*

Philip Lessner and John Newman
Applied Science Division
Lawrence Berkeley Laboratory
and
Department of Chemical Engineering
University of California
Berkeley, California 94720

August 1983

* This work was supported by the Assistant Secretary for Conservation and Renewable Energy, Office of Energy Systems Research, Energy Storage Division of the U.S. Department of Energy under Contract No. DE-AC03-76SF00098.

Hydrodynamics and Mass Transfer in a Porous-Wall Channel

Philip Lessner and John Newman
Applied Science Division
Lawrence Berkeley Laboratory
and
Department of Chemical Engineering
University of California
Berkeley, California 94720

August 1983

Abstract

The hydrodynamics and mass-transfer equations for a porous-wall flow channel have been solved over a large range of Re and Sc. Jorne has analyzed the low Re, high Sc case. For the high Re, high Sc case we find that $\frac{\tau_{xy} h^2}{\mu x v_w} = 2.43 \mathrm{Re}^{0.5}$ and $Nu = 0.8277 \mathrm{Re}^{0.5} Sc^{1/3}$ at the solid wall. The intermediate range is treated by numerical methods.

Introduction

A flow channel with flow entering through a porous wall may find use in practical electrochemical cells (1). Previously, Jorne (2) has solved the governing fluid dynamic and mass transfer equations for small and uniform wall Reynolds number by a regular peturbation technique. When the end of the channel is closed off, the mass transfer boundary layer that forms on the solid electrode opposite the porous wall is of constant thickness. Only a few other electrodes (e.g. the rotating disk and the impinging jet) show a uniformly accessible surface. Therefore, this arrangement is of theoretical as well as practical interest.

We have extended Jorne's work to cover moderate and large as well as small Re. At high Re a hydrodynamic boundary layer is formed near the solid wall. This allows us to apply powerful singular peturbation techniques as Re$\to\infty$. We also obtain a numerical solution valid over the entire range of Re. Jorne's solution is valid at small Re. By combining all these results, we are able to picture the flow over the entire range of Re.

A similar analysis is done for the mass transfer. However, we have confined our theoretical work to high Sc -- which is the region of most interest in liquid phase mass transfer. Our numerical results show where the high Sc asymptote is valid.

Hydrodynamics

We take the origin of the coordinates to be at the solid wall, in the center of a flow channel which extends for a large distance in both directions (Figure 1). The flow is two dimensional and is described by the Navier-Stokes equations:

$$v_x \frac{\partial v_x}{\partial x} + v_y \frac{\partial v_x}{\partial x} = \frac{-1}{\rho}\frac{\partial P}{\partial x} + \nu\left(\frac{\partial^2 v_x}{\partial x^2} + \frac{\partial^2 v_x}{\partial y^2}\right) \quad (1)$$

$$v_y \frac{\partial v_y}{\partial x} + v_y \frac{\partial v_y}{\partial y} = \frac{-1}{\rho}\frac{\partial P}{\partial y} + \nu\left(\frac{\partial^2 v_y}{\partial x^2} + \frac{\partial^2 v_y}{\partial y^2}\right) \quad (2)$$

and the equation of continuity:

$$\frac{\partial v_x}{\partial x}+\frac{\partial v_y}{\partial y}=0 \tag{3}$$

The boundary conditions are:

$$at\ \ y=0,\ \ v_x=0 \text{ and } v_y=0 \tag{4a}$$

$$at\ \ y=h,\ \ v_x=0 \text{ and } v_y=-v_w \tag{4b}$$

The boundary conditions and the equation of continuity suggest the following form for the velocity components:

$$v_y=Q(y) \tag{5a}$$

$$v_x=-xQ'(y) \tag{5b}$$

After substituting Equations (5) into Equations (1) and (2) and taking the curl to eliminate pressure, Jorne obtained the following equation for Q

$$Q'Q''-QQ'''=-\nu Q^{iv} \tag{6}$$

with the boundary conditions

$$at\ \ y=0,\ \ Q'=0 \text{ and } Q=0 \tag{7a}$$

$$at\ \ y=h,\ \ Q'=0 \text{ and } Q=-v_w \tag{7b}$$

It is convienient to put Equations (6) and (7) into dimensionless form by introducing the following dimensionless quantities

$$R=\frac{Q}{v_w} \tag{8}$$

$$Re=\frac{v_w h}{\nu} \tag{9}$$

$$\gamma=\frac{y}{h} \tag{10}$$

Then we obtain

$$R'R''-RR'''=\frac{-1}{\text{Re}}R^{iv} \tag{11}$$

with boundary conditions

$$at\ \ \gamma=0,\ \ R'=0 \text{ and } R=0 \tag{12a}$$

$at\ \gamma=1,\ R'=0$ and $R=-1$ **(12b)**

At low Re, Jorne showed that there is a regular peturbation problem. The first few terms in the regular peturbation expansion have been obtained by Jorne (2). In the limit as Re becomes infinite, we lose the fourth derivative, and the problem becomes singular. Peturbation expansions need to be developed for both inner and outer regions. In the region of intermediate Re neither the low nor high Re expansions is adequate, and we need to obtain a numerical solution of the complete equation.

The full equation is a non-linear, two-point boundary value problem. It has been solved by reducing it to two second order equations and linearizing them about a trial solution. The linearized equations were solved by BAND, a subroutine developed by Newman (3). Figure 2a shows the velocity profile at a high Re.

To begin our singular peturbation expansion we start with the outer region. In this region our variable is denoted by:

$$\tilde{y}=y \qquad (13)$$

The differential equation for the first term in the outer region is:

$$\tilde{R}'_0\tilde{R}''_0=\tilde{R}_0\tilde{R}'''_0 \qquad (14)$$

with the boundary conditions

$$at\ \gamma=0,\ \tilde{R}_0=0 \qquad (15a)$$

$$at\ \gamma=1,\ \tilde{R}'_0=0 \text{ and } \tilde{R}_0=-1 \qquad (15b)$$

The solution to this nonlinear problem turns out to be remarkably simple:

$$\tilde{R}_0=-sin(\pi\frac{\gamma}{2}) \qquad (16)$$

At high Re, order of magnitude analysis shows that the proper form of the stretched distance in the inner region is:

$$\bar{y}=\frac{y\sqrt{\text{Re}}}{h} \qquad (17)$$

The inner flow variable is:

$$\bar{R}=\frac{Q\sqrt{\mathrm{Re}}}{v_w} \tag{18}$$

This leads to the following differential equation for the first term in the inner solution:

$$-\bar{R}'_0\bar{R}''_0+\bar{R}_0\bar{R}'''_0=-\bar{R}^{iv}_0 \tag{19}$$

with the boundary conditions:

$$at \quad \bar{y}=0, \quad \bar{R}_0=0 \text{ and } \bar{R}'_0=0 \tag{20}$$

By requiring that:

$$\lim_{\bar{y}\to\infty}\bar{R}=\lim_{\tilde{y}\to 0}\tilde{R} \tag{21}$$

we can determine the matching conditions as $\bar{y}$ tends toward infinity

$$\bar{y}\to\infty \quad \bar{R}_0\to-\frac{\pi}{2} \quad \bar{R}'_0\to 0 \tag{22}$$

The method of solution of Equation (19) subject to boundary conditions (20) and matching condition (22) is similar to that of the full equation. Figure 2b shows the boundary layer in more detail.

The shear stress at the solid wall can be written as a function of Re:

$$\frac{\tau_{xy}h^2}{\mu x v_w}=G(Re) \tag{23}$$

Our boundary layer solution yields:

$$G(Re)=2.43\mathrm{Re}^{0.5} \tag{24}$$

Jorne's low Re peturbation solution yields the following

$$G(Re)=6+\frac{16\mathrm{Re}}{35} \tag{25}$$

Figure 3 shows a plot of G(Re) vs. Re as determined by the full numerical solution. The low and high Re asymptotes are also plotted. For Re<1 the low Re asymptote is a good approximation to the shear stress, while for Re>500 the high Re line fits the data well. Reynolds numbers between 1 and 500 are in the intermediate region.

Mass Transfer

Since v_y is a function of y only, the equation of convective diffusion can be written as:

$$v_y \frac{dc_i}{dy} = D_i \frac{d^2 c_i}{dy^2} \tag{26}$$

For our problem the boundary conditions take the form:

$$at \quad y=0, \ \ c_i = c_o \tag{27a}$$

$$at \quad y=h, \ \ c_i = c_b \tag{27b}$$

Equations (25) and (26) can be put in dimensionless form by introducing a dimensionless concentration

$$\Theta = \frac{c_i - c_o}{c_b - c_o} \tag{28}$$

Then:

$$\frac{d^2\Theta}{d\gamma^2} - Pe R(\gamma) \frac{d\Theta}{d\gamma} = 0 \tag{29}$$

with boundary conditions:

$$at \quad \gamma=0, \ \ \Theta=0 \tag{30a}$$

$$at \quad \gamma=1, \ \ \Theta=1 \tag{30b}$$

The solution to this equation can be represented as an integral

$$\Theta = \frac{\int_0^{\gamma} e^{Pe\int_0^{\beta} R(\alpha)d\alpha} d\beta}{\int_0^{1} e^{Pe\int_0^{\beta} R(\alpha)d\alpha} d\beta} \tag{31}$$

The Nussult number is simply:

$$Nu = \left.\frac{d\Theta}{d\gamma}\right|_{\gamma=0} = \frac{1}{\int_0^{1} e^{Pe\int_0^{\gamma} R(\alpha)d\alpha} d\gamma} \tag{32}$$

The number of points in the integration is dependent on the number of intervals used in the hydrodynamic solution. A finer mesh would be appropriate for the mass transfer problem at high Pe, but this is limited by computer memory size. At high Pe, the exponential in the integral of Equation (31) will change rapidly. We need to interpolate between grid points.

To do this interpolation we first stretch the distance with Sc:

$$\xi=\gamma Sc^{1/3} \tag{33}$$

Then Equation (31) takes the form

$$Nu=\frac{Sc^{1/3}}{\int_0^{Sc^{1/3}} e^{ReSc^{2/3}\int_0^{\gamma'} R(\xi)d\xi} d\gamma'} \tag{34}$$

At distances close to the solid wall we can write v_x in the form of a truncated Taylor series:

$$v_x=\beta(x)y \tag{35}$$

$$\beta(x)=-\frac{\tau_{xy}}{\mu}\bigg|_{y=0} \tag{36}$$

From Equation (3) v_y becomes

$$v_y=-\tfrac{1}{2}\beta'(x)y^2 \tag{37}$$

This form for the y velocity suggests that we interpolate quadratically between grid points.

At high Sc a mass transfer boundary layer forms. Then the concentration can be represented as

$$\Theta=\int_0^{\eta} e^{-x^3}dx \tag{38}$$

where

$$\eta=y\frac{\sqrt{\beta}}{(9D_i\int_0^{x}\sqrt{\beta}dx)^{1/3}} \tag{39}$$

The high Schmidt number asymptote can be constructed with a knowledge of G(Re) from Figure 3. Thus:

$$Nu_{Sc\to\infty}=0.6160(G(Re))^{1/3}Pe^{1/3} \quad \textbf{(40)}$$

Using this representation, Jorne (2) obtained for low Re, high Sc cases:

$$Nu=1.12(1+\frac{8}{108}Re)^{1/3}Pe^{1/3} \quad (41)$$

In the limit as Re $\rightarrow$ 0 this yields

$$Nu=1.12\mathrm{Re}^{1/3}Sc^{1/3} \quad (42)$$

Using our results for the hydrodynamics at high Re we obtain for the high Re, high Sc asymptote

$$Nu=0.8277\sqrt{\mathrm{Re}}Sc^{1/3} \quad (43)$$

The high Sc asymptote over the whole range of Re can be constructed from Equation (40) and Figure 3. At finite Sc the actual value of Nu will deviate from this asymptote. Figure 4 shows the correction to be applied to the asymptote at finite Sc.

References

(1) J. Jorne, "Flow Distribution in the Zinc-Chloride Battery", *Journal of the Electrochemical Society, 129*, (10), 2251, (1982)

(2) J. Jorne, "Mass Transfer in a Laminar Flow Channel With Porous Wall", *Journal of the Electrochemical Society, 129*, (8), 1727, (1982)

(3) John Newman, *Electrochemical Systems*, Englewood Cliffs,Prentice-Hall, Inc., 1973

Nomenclature

Roman Letters

c,concentration,$mol\ m^{-3}$

D, diffusion coefficient, $m^2 s^{-1}$

$G(Re)$, see Equation 23 and Figure 3.

h, spacing between porous and solid wall, m.

N, molar flux, $mol\ m^{-2} s^{-1}$.

Nu, Nusselt number,$N_i h / D_i \Delta c$.

P, dynamic pressure, Pa.

Pe, Peclet number, $v_w h / D$.

Q, defined by Equation 5, $m\ s^{-1}$.

R, dimensionless velocity.

Re, Reynolds number, $v_w h / \nu$.

Sc, Schmidt number, ν / D

v, velocity, $m\ s^{-1}$.

x, coordinate along wall, m.

y, coordinate perpendicular to wall, m.

Greek Letters

$\beta(x)$, defined by Equation 34, s^{-1}.

γ, dimensionless distance.

η, defined by Equation 39.

Θ, dimensionless concentration.

μ, dynamic viscosity, $kg\ m^{-1} s^{-1}$.

ν, kinematic viscosity, $m^2 s^{-1}$.

ξ, stretched distance.

π, 3.14.

ρ, density, $kg\ m^{-3}$.

τ, shear stress, $nt\ m^{-2}$.

Diacritical Marks

$\bar{}$, inner variable.

~, outer variable.

Superscripts

$'$, first derivative.

$''$, second derivative.

$'''$, third derivative.

iv, fourth derivative.

Subscripts

i, species.

o, first term.

w, wall.

x, x direction.

y, y direction.

Acknowledgement

This work was supported by the Assistant Secretary for Conservation and Renewable Energy, Office of Energy Systems Research, Energy Storage Division of the U.S. Departement of Energy under Contract No. DE-AC03-76SF00098.

List of Figures

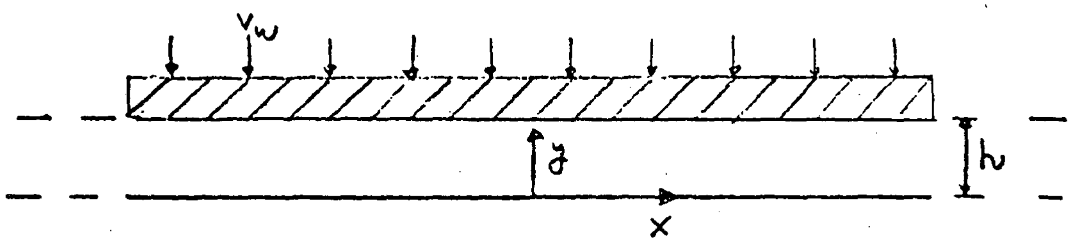

Fig. 1

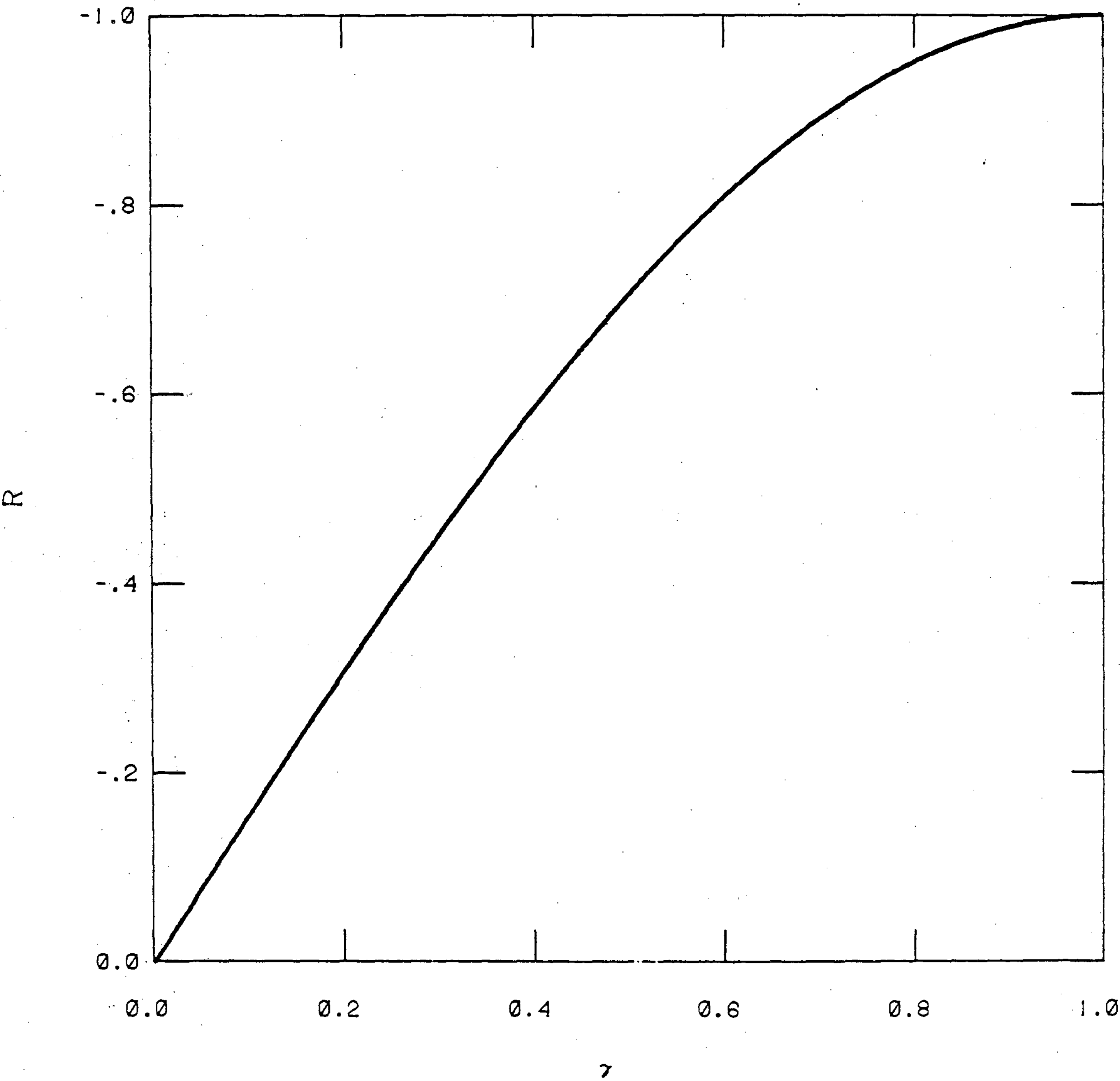

Fig. 2a

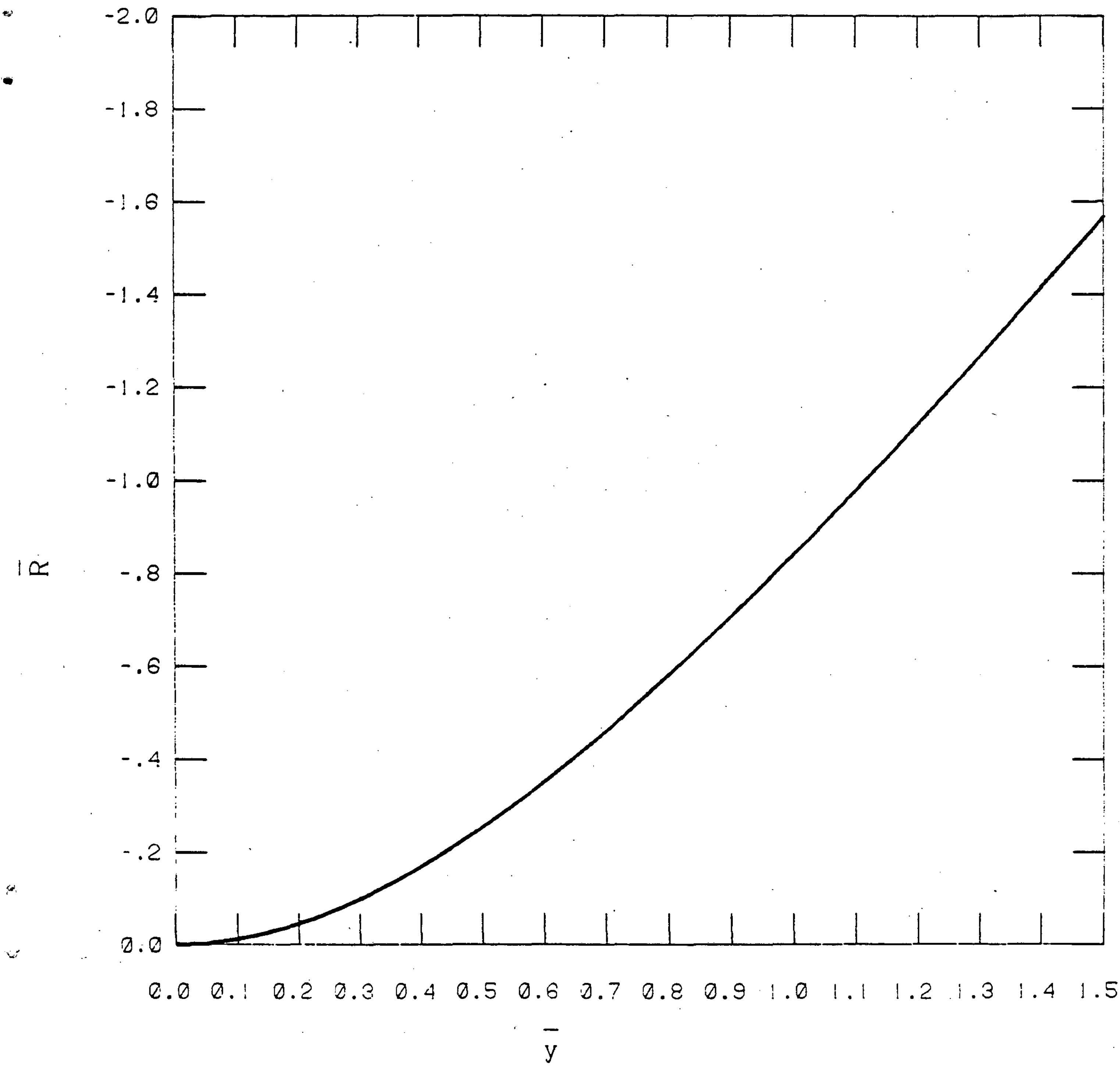
-2.0
-1.8
-1.6
-1.4
-1.2
-1.0
-.8
-.6
-.4
-.2
0.0
R̄
0.0 0.1 0.2 0.3 0.4 0.5 0.6 0.7 0.8 0.9 1.0 1.1 1.2 1.3 1.4 1.5
ȳ

Fig. 2b

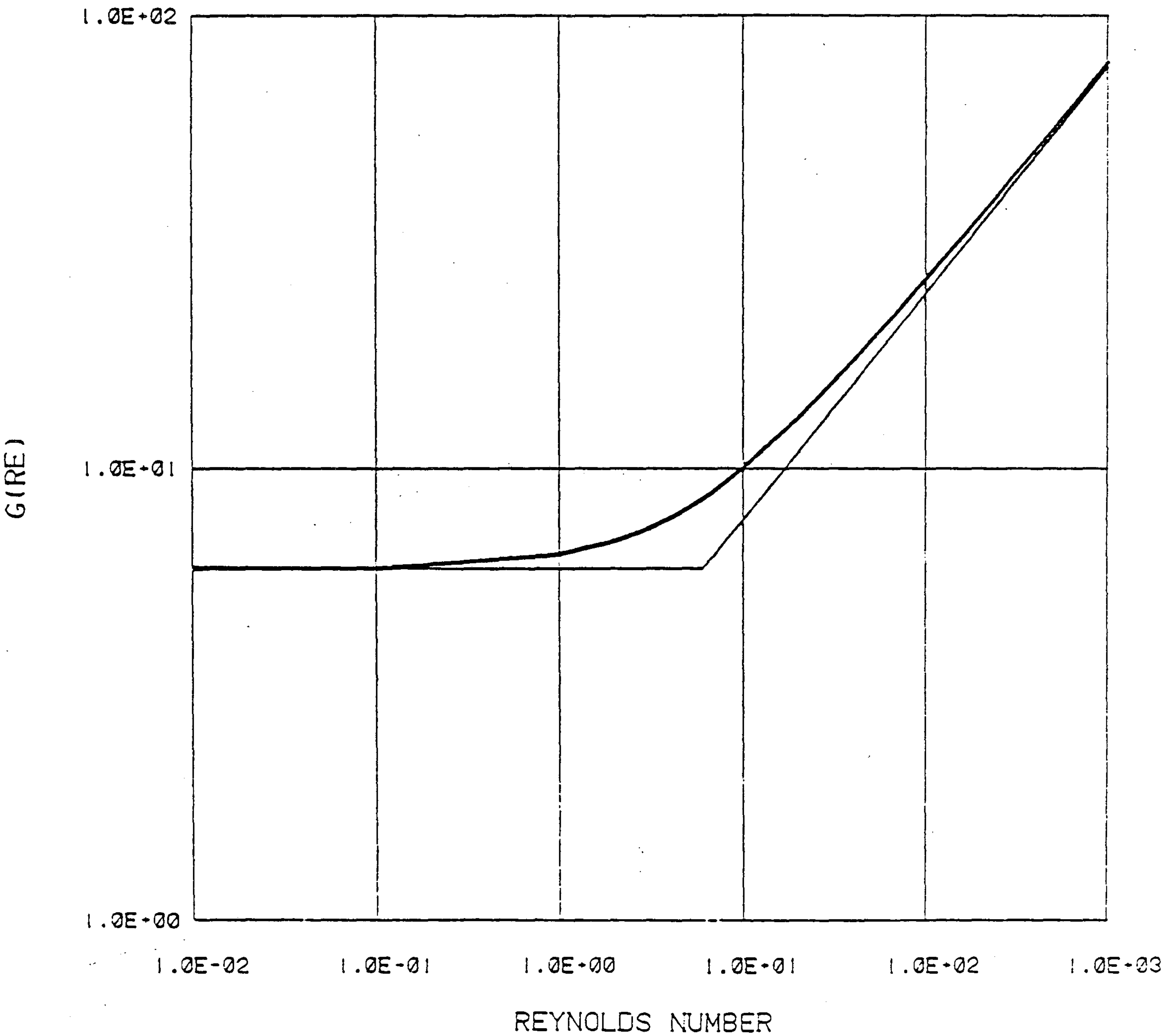
1.0E+02
1.0E+01
1.0E+00
G(RE)
1.0E-02
1.0E-01
1.0E+00
1.0E+01
1.0E+02
1.0E+03
REYNOLDS NUMBER

Fig. 3

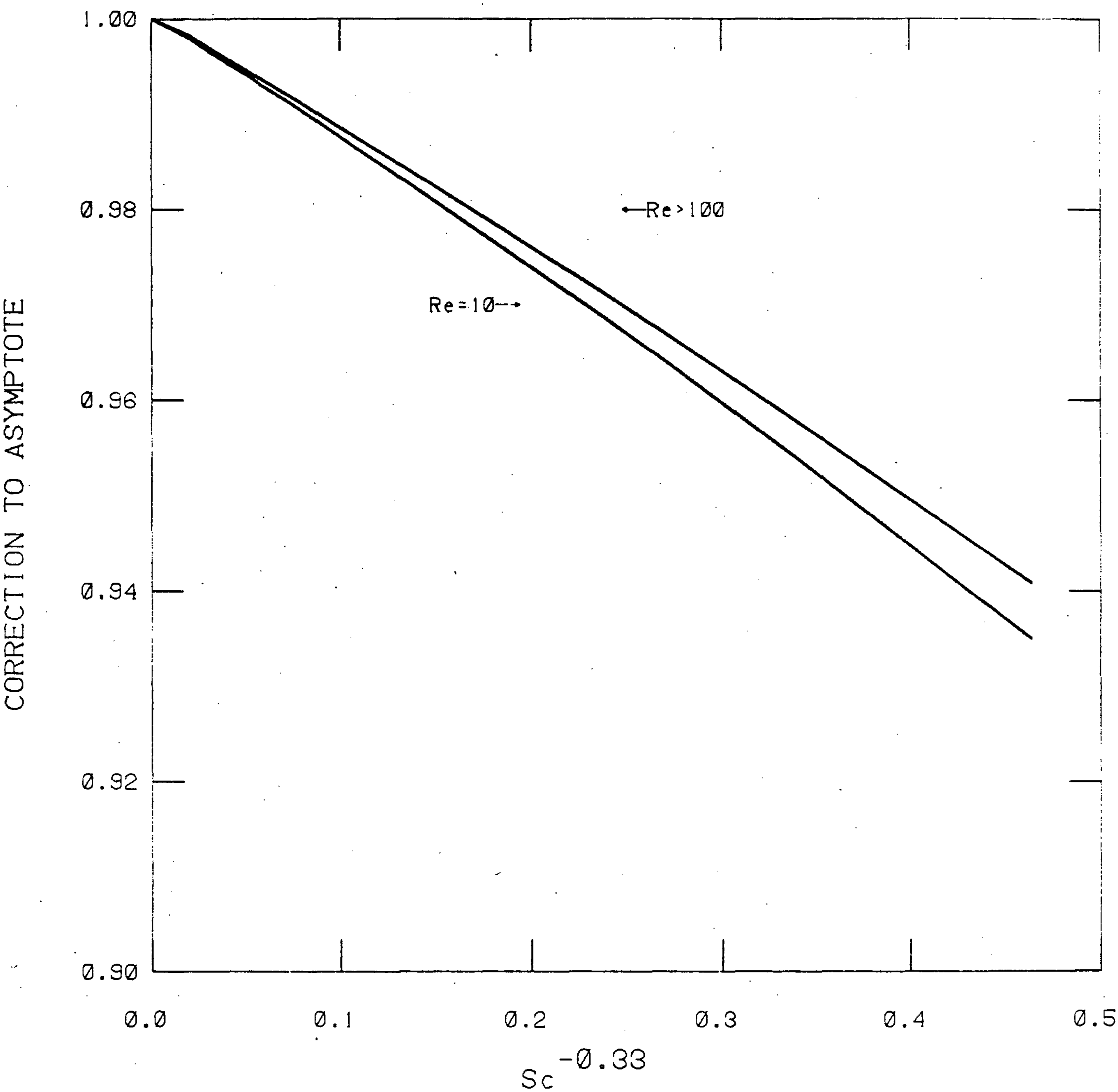
1.00
0.98
0.96
0.94
0.92
0.90
CORRECTION TO ASYMPTOTE
←Re>100
Re=10→
0.0
0.1
0.2
0.3
0.4
0.5
Sc^-0.33

Fig. 4a

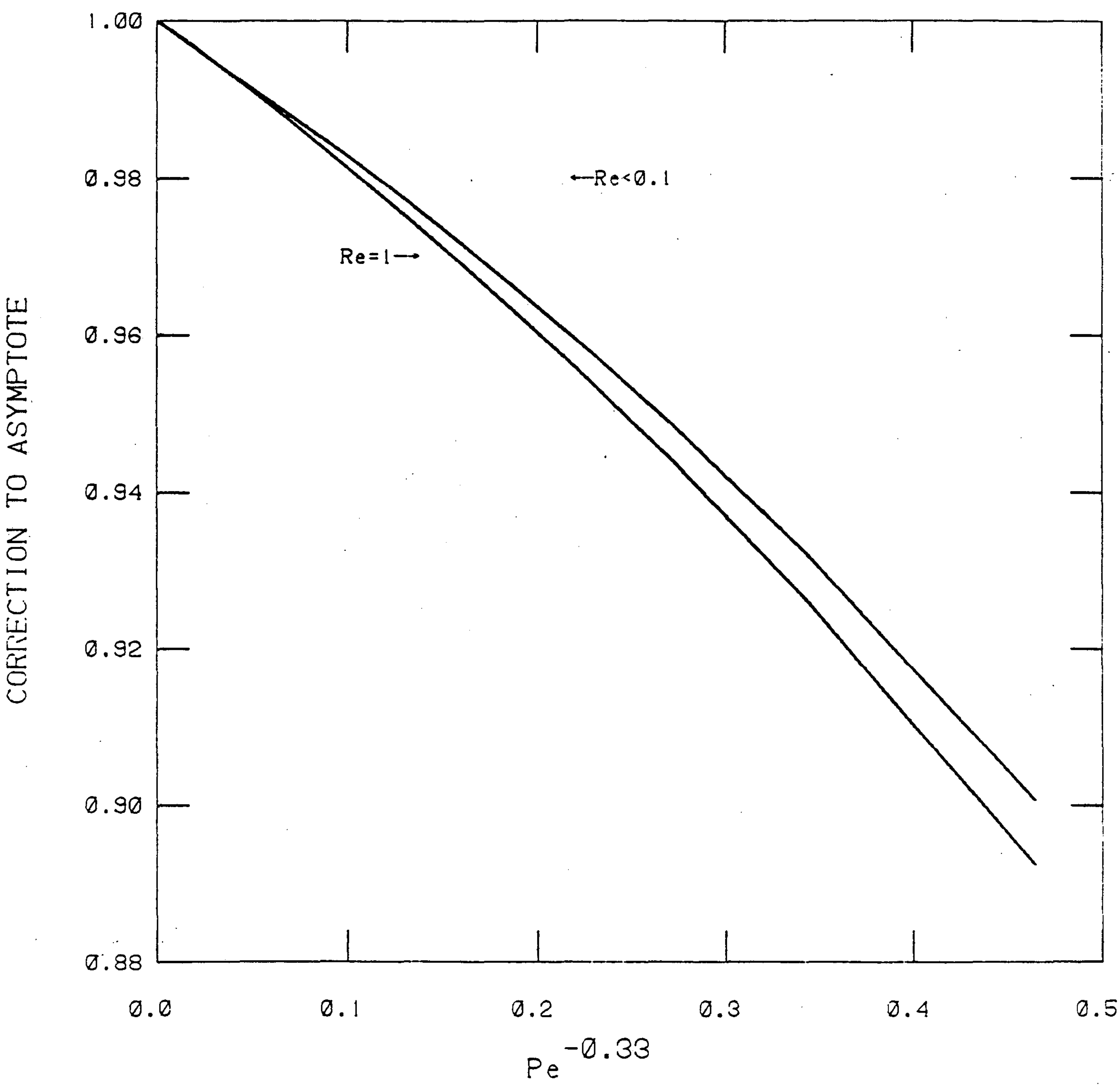
1.00
0.98
0.96
0.94
0.92
0.90
0.88
0.0
0.1
0.2
0.3
0.4
0.5
←Re<0.1
Re=1→
CORRECTION TO ASYMPTOTE
Pe^-0.33

Fig. 4b

TECHNICAL INFORMATION DEPARTMENT
LAWRENCE BERKELEY LABORATORY
UNIVERSITY OF CALIFORNIA
BERKELEY, CALIFORNIA 94720